Detection of *Nα*-terminally formylated native proteins by a pan-*N*-formyl methionine-specific antibody

Received for publication, November 4, 2022, and in revised form, March 3, 2023 Published, Papers in Press, March 27, 2023,
https://doi.org/10.1016/j.jbc.2023.104652

Dasom Kim[1], Ok-Hee Seok[1], Shinyeong Ju[2], Sang-Yoon Kim[1], Jeong-Mok Kim[3], Cheolju Lee[2,4], and Cheol-Sang Hwang[5,*]

From the [1]Department of Life Sciences, Pohang University of Science and Technology, Pohang, Republic of Korea; [2]Chemical & Biological Integrative Research Center, Korea Institute of Science and Technology, Seoul, Republic of Korea; [3]Department of Life Science, Hanyang University, Seoul, Republic of Korea; [4]Division of Bio-Medical Science & Technology, KIST School, Korea University of Science and Technology, Seoul, Republic of Korea; [5]Department of Life Sciences, Korea University, Seoul, Republic of Korea

Reviewed by members of the JBC Editorial Board. Edited by Chris Whitfield

***N*-formyl methionine (fMet)-containing proteins are produced in bacteria, eukaryotic organelles mitochondria and plastids, and even in cytosol. However, *Nα*-terminally formylated proteins have been poorly characterized because of the lack of appropriate tools to detect fMet independently of downstream proximal sequences. Using a fMet-Gly-Ser-Gly-Cys peptide as an antigen, we generated a pan-fMet-specific rabbit polyclonal antibody called anti-fMet. The raised anti-fMet recognized universally and sequence context–independently Nt-formylated proteins in bacterial, yeast, and human cells as determined by a peptide spot array, dot blotting, and immunoblotting. We anticipate that the anti-fMet antibody will be broadly used to enable an understanding of the poorly explored functions and mechanisms of Nt-formylated proteins in various organisms.**

Nα-terminal (Nt-) formylation of cellular proteins is a pretranslational modification that occurs before protein synthesis in ribosomes. Specifically, methionyl-tRNA formyltransferase (FMT) transfers a formyl moiety from 10-formyltetrahydrofolate to the free α-amino group of initiator Met-tRNAi. *N*-formyl methionine (fMet)-tRNAi is recruited to yield Nt-formylated polypeptides by bacterial and bacterial-type ribosomes (1–7). The resulting formyl group of the Nt-fMet-containing polypeptide is cotranslationally removed by ribosome-associated peptide deformylase (PDF) (8–12). Crucially, the production of Nt-formylated proteins had been previously hypothesized to be confined to bacteria and bacteria-originated eukaryotic organelles mitochondria and plastids. In contrast to this general hypothesis, our previous study revealed that fMet-mediated protein synthesis occurs even in the cytosol of the budding yeast *Saccharomyces cerevisiae*, a simple eukaryotic organism (13, 14). Cytosolic Nt-formylated proteins increase the adaptability of yeast cells to undernutrition and cold stress. Nt-formylated proteins are removed by a eukaryotic fMet/N-degron pathway that recognizes Nt-fMet of proteins as a specific degradation signal, termed fMet/N-degron (Fig. S1) (13). It is noteworthy that fMet/N-degrons also occur in bacteria, but the bacterial recognition components of fMet/N-degrons remain to be identified (15).

In addition to these fundamental roles in protein synthesis and degradation, bacterial and mitochondrial Nt-formylated proteins are sources of N-formyl peptides that elicit immune responses *via* formyl peptide receptor–mediated signaling pathways (16–18). Nt-formylation on mitochondrial DNA–encoded proteins substantially contributes to the steady-state level and organization of oxidative phosphorylation complexes (19, 20). Furthermore, multiple age-associated diseases, including cardiovascular disorders, have a positive correlation to blood fMet levels through an as-yet-unknown pathway(s) (21). Consequently, Nt-formylation greatly expands the functional and mechanistic complexities of the cellular proteome (12, 13, 22) and plays pivotal roles in a vast range of physiological and pathological processes. However, the lack of appropriate tools to simultaneously detect diverse Nt-formylated proteins independent of mass spectrometry has hampered our understanding of the extent, dynamics, and functions of Nt-formylation in native proteomes.

Some antibodies against specific fMet-containing peptides have been developed to detect several Nt-formylated proteins or Nt-formylated peptides (13, 23). Nonetheless, their applications are restricted to only a few proteins with fMet-containing peptides that are the same or very similar to the antigen fMet-peptides. The use of pan-specific antibodies allows the characterization of proteins with desired chemical modifications (24–26). However, to the best of our knowledge, a pan-specific antibody against fMet has not been reported.

Results

Generation of a pan-fMet-specific antibody

The lack of adequate tools to simultaneously detect fMet-containing proteins led us to develop pan-fMet–specific antibodies. In attempts to raise the fMet-specific antibodies, we employed the synthetic fMet-Gly-Ser-Gly-Cys (fMGSGC) peptide as an antigen (Fig. 1*A*). Notably, the fMGSGC peptide includes the tripeptide Gly-Ser-Gly as a linker which has good

* For correspondence: Cheol-Sang Hwang, hwangcs@korea.ac.kr.

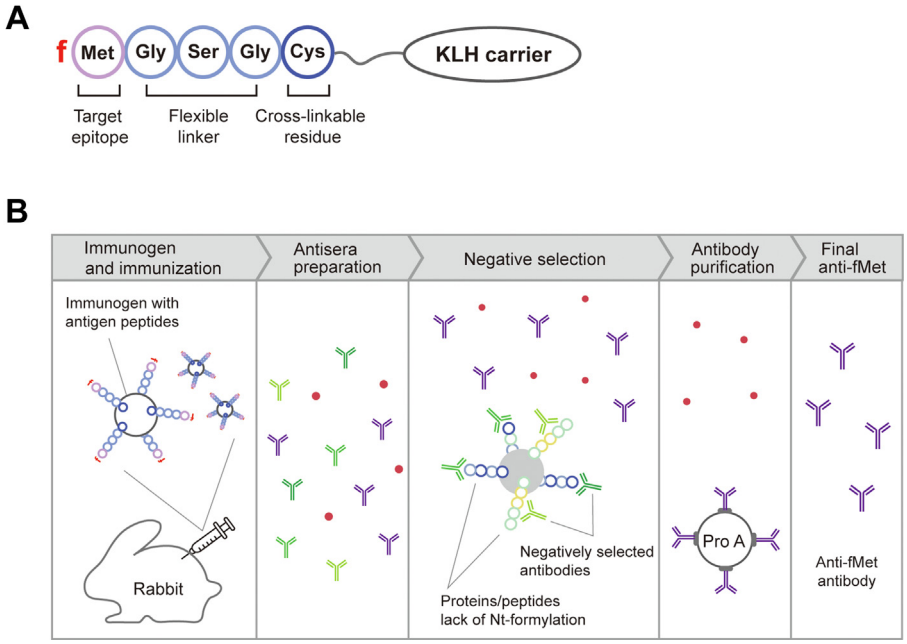

Figure 1. Schematic representation of the development of a pan-fMet-specific antibody. *A*, synthetic fMGSGC-peptide antigen for generation of a pan-fMet-specific (anti-fMet) antibody. The fMGSGC antigen contains Nt-formylated fMet, a flexible GSG linker, a thiol-based conjugatable Cys, and a KLH carrier protein. *B*, scheme for anti-fMet generation. Anti-fMet antibodies were induced by immunization of rabbits with the fMGSGC antigen, followed by antisera preparation, negative selection-based removal of nonspecific antisera, and subsequent protein A-affinity chromatography. fMet, N-formyl methionine; fMGSGC, fMet-Gly-Ser-Gly-Cys; GSG, Gly-Ser-Gly; KLH, keyhole limpet hemocyanin.

flexibility (27) and lower immunogenicity than other peptide linkers owing to its shorter side chains (28). The C-terminal Cys of fMGSGC was used for thiol-based conjugation of the peptide to the keyhole limpet hemocyanin carrier protein (Fig. 1*A*).

Rabbit polyclonal antisera against the fMGSGC peptide were produced as described in previous studies (13, 29). Nonspecific antibodies were negatively selected from the antisera using affinity chromatography gels that were conjugated with extracts from human HeLa cervical cancer cells overexpressing *Escherichia coli* PDF (*Ec*PDF) or *fmt1Δ S. cerevisiae* cells lacking Fmt1 formyltransferase. *Ec*PDF expression or *fmt1* deletion was introduced to maximally remove endogenously Nt-formylated proteins in human or yeast cells, respectively. The flowthrough fractions of sera following negative selection were concentrated by protein A–based affinity chromatography to yield anti-fMet^{Hs} and anti-fMet^{Sc} (superscripts denote the origin of the cell extracts used for negative selection. *Hs*, *Homo sapiens*; *Sc*, *S. cerevisiae*) (Fig. 1*B*).

Specificity of anti-fMet antibody in vitro

To determine the specificity and sequence-context independence of the raised anti-fMet^{Hs}, we first employed SPOT peptide arrays (30). In this assay, XZ-D2$^{3-11}$ peptides included X (M, Nt-unmodified Met; fM, Nt-formylated Met; AcM, Nt-acetylated Met), Z (any 20 amino acids), and D2$^{3-11}$ (Ile-Ala-Ile-Gly-Thr-Tyr-Gln-Glu-Lys: IAIGTYQEK, identical residues at position 3 to 11 of the previously characterized *Chlamydomonas reinhardtii* chloroplast D2 protein) (13, 15). The XZ-D2$^{3-11}$ peptides were C-terminally attached to a SPOT membrane at the same concentration and tested for binding to anti-fMet^{Hs} (Fig. 2*A*). The SPOT assay indicated that anti-fMet^{Hs} bound preferentially to Nt-formylated fMZ-D2$^{3-11}$ peptides but not noticeably to Nt-unmodified MZ-D2$^{3-11}$ or Nt-acetylated AcMZ-D2$^{3-11}$ peptides (Fig. 2*A*).

To confirm the broad specificity of anti-fMet^{Hs} to fMet-containing peptides independent of the fMet-proximal sequence context, we also performed dot blot assays using a set of peptides. For these assays, X-Pin4$^{2-11}$ or X-Yjl068c$^{2-11}$ peptides consisted of X (M, fM, or AcM) and identical residues at position 2 to 11 of the previously characterized yeast Nt-formylated RNA-binding protein Pin4 (Glu-Thr-Ser-Ser-Phe-Gln-Asn-Gly-Ser-Lys: ETSSFQNGSK) or the yeast esterase protein Yjl068c (Lys-Val-Val-Lys-Glu-Phe-Ser-Gly-Ser-Lys: LVVKEFSGSK), respectively (13). In line with the results of the above SPOT assay, these dot blot analyses with X-Pin4$^{2-11}$ and X-Yjl068c$^{2-11}$ indicated that anti-fMet^{Hs} preferentially bound to Nt-formylated fMet-containing peptides but not to Nt-unmodified Met-containing peptides or Nt-acetylated AcMet-containing peptides (Fig. 2, *B* and *C*).

To investigate the preferential binding of anti-fMet^{Hs} to Nt-formylated proteins over their unformylated counterparts, we also purified the previously characterized C-terminally glutathione-S-transferase (GST)-tagged MD-D2$^{3-11}$-GST and the C-terminally HA-His6-tagged RNA polymerase II mediator complex protein Pgd1$_{HA\text{-}His6}$ from *E. coli* in the presence or absence of PDF inhibitor actinonin (13). Indeed, treatment with actinonin produced Nt-formylated fMD-D2$^{3-11}$-GST and fPgd1$_{HA\text{-}His6}$ as determined by immunoblotting with the anti-fMet^{Hs} antibody (Fig. 3, *A* and *B*).

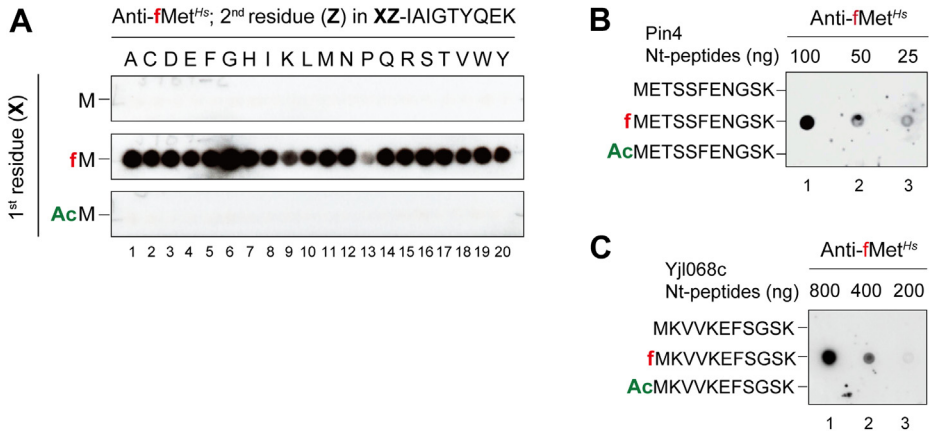

Figure 2. Broad binding specificity of anti-fMet for various Nt-formylated peptides. *A*, immunoblotting with the anti-fMet^{Hs} antibody purified through negative selection with HeLa cell lysates and SPOT peptide arrays with 11-residue peptides XZ-IAIGTYQEK (XZ-D2$^{3-11}$; X represents Met, fMet, or AcMet, Z is one of 20 amino acids, and D2$^{3-11}$ is derived from the 3–11 residues of *C. reinhardtii* D2 protein). *B*, dot immunoblotting with the anti-fMet^{Hs} antibody *versus* decremental amounts of the unmodified METSSENGSK peptide (11 Nt-residues of *S. cerevisiae* Pin4) and either its Nt-formylated or Nt-acetylated counterpart. *C*, same as (*B*), but with the MKVVKEFSGSK peptide (11 Nt-residues of *S. cerevisiae* Yjl068c). See also main text and Experimental procedures. *A–C* images are representative of two independent experiments. fMet, N-formyl methionine.

To further corroborate the specificity of anti-fMet^{Hs}, we next performed an *in vitro* deformylation assay using purified wildtype *Ec*PDF$_{His6}$ or catalytically inactive *EcPDF*$^{E134A}_{His6}$ with substitution of Glu134 with Ala and its substrate fMD-D2$^{3-11}$-GST or fPgd1$_{HA-His6}$. As expected, the levels of Nt-formylated fMD-D2$^{3-11}$-GST and fPgd1$_{HA-His6}$ were markedly decreased in the presence of *Ec*PDF$_{His6}$, but not of *EcPDF*$^{E134A}_{His6}$ (Fig. 3, *C* and *D*). The incomplete deformylation of substrate proteins observed here might result from the oxygen-mediated inactivation of purified *Ec*PDF$_{His6}$ (31) or from the structural inaccessibility of their fMet by purified *Ec*PDF$_{His6}$ since the binding of *Ec*PDF to the ribosome is required for the efficient deformylation of the fMet-containing nascent polypeptides (10).

The specificity of anti-fMet^{Hs} was also verified by observing noticeable quenching of immunoblotting signals by Nt-formylated fMet amino acid but not by Nt-unmodified free Met or Nt-acetylated AcMet amino acid (Fig. 3*E*). The observed incomplete quenching by fMet amino acid indicated that anti-fMet^{Hs} might have a higher binding affinity to the fMet present in proteins than fMet amino acid. Further, immunoblotting with anti-fMet^{Hs} and serially diluted fMD-D2$^{3-11}$-GST or fPgd1$_{Ha-His6}$ revealed that the detection limit of anti-fMet^{Hs} for those proteins was ∼6.4 ng or ∼1.6 ng, respectively (Fig. 3, *F* and *G*). Taken together, we raised anti-fMet^{Hs} that recognized, specifically and sensitively, fMet-containing proteins independent of the fMet-proximal sequence contexts *in vitro*.

Detection of Nt-formylated native proteins in E. coli *using anti-fMet^{Hs}*

Nearly all nascent polypeptides in bacteria contain pre-translationally generated Nt-fMet residues that can be cotranslationally deformylated by ribosome-associated PDFs (10, 22). To directly verify the PDF-mediated deformylation of nascent proteins, actinonin-susceptible *ΔarcAB E. coli* cells (32) were cultured in the absence or presence of actinonin for 0, 1, and 3 h at 37 °C, followed by preparation of cell extracts and immunoblotting with anti-fMet^{Hs} (Fig. 4*A*). As expected, actinonin treatment greatly increased both the species and amounts of Nt-formylated proteins in *ΔarcAB E. coli* cells, validating the utility of anti-fMet^{Hs} to monitor the expression of fMet-bearing proteins in bacteria (Fig. 4*A*).

Detection of Nt-formylated native proteins in S. cerevisiae *using anti-fMet^{Sc}*

By immunoblotting with anti-MD-D2^{fMet} that specifically recognized Nt-formylated fMD-D2, we previously showed that overexpression of *S. cerevisiae* Fmt1^{ΔSP} (*Sc*Fmt1^{ΔSP} lacking mitochondrion-targeting signal peptide) dramatically increases the levels of Nt-formylated fMD-D2$^{3-11}$-GST in the cytosol of yeast *S. cerevisiae* cells (13). Similarly, immunoblotting with anti-fMet^{Sc} revealed that overexpression of *Sc*Fmt1^{ΔSP} strongly upregulated a wide range of Nt-formylated native proteins in yeast *fmt1Δ* cells (Fig. 4*B*). This effect was almost abolished by co-expression of wildtype *Ec*PDF but not catalytically inactive *Ec*PDF^{E134A} (Fig. 4*B*). These results allowed the use of anti-fMet^{Sc} to detect Nt-formylated native proteins in yeast cells.

Detection of Nt-formylated native proteins in human cell lines using anti-fMet^{Hs}

The production of multiple Nt-formylated proteins by cytosolic ribosomes has been demonstrated in *S. cerevisiae* (13), but its occurrence in mammals and other multicellular eukaryotes has not been explored. Therefore, we co-expressed C-terminally triple flag-tagged EcFMT$_{3f}$ together with either wildtype EcPDF$_{3f}$ or catalytically inactive *EcPDF*$^{E134A}_{3f}$ in the cytosol of HeLa cells. Anti-fMet^{Hs}-based immunoblotting revealed that overexpression of *Ec*FMT$_{3f}$ dramatically upregulated Nt-formylated native proteins in HeLa, which was almost abolished by co-expression of *Ec*PDF$_{3f}$, but not *EcPDF*$^{E134A}_{3f}$ (Fig. 4*C*). Thus, we concluded that cytosolic

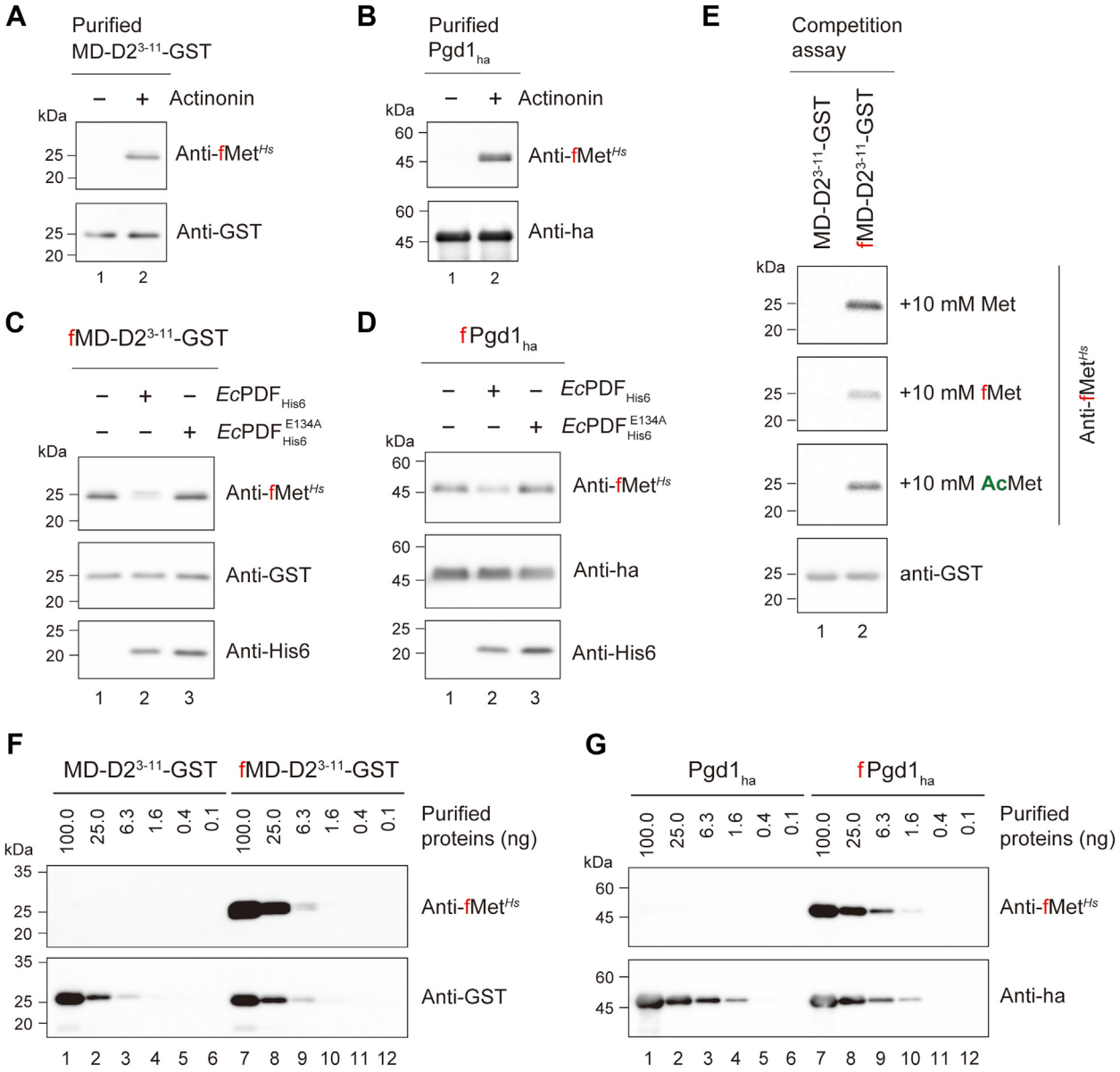

Figure 3. Broad binding specificity of anti-fMet for various Nt-formylated proteins. *A*, immunoblotting with anti-fMet^{Hs} and 0.2 μg MD-D2$^{3-11}$-GST purified from *E. coli* cells with or without 2 μg/ml actinonin treatment. *B*, same as (*A*), but with 0.2 μg Pgd1$_{HA-His6}$. *C*, immunoblotting with anti-fMet^{Hs} and 1 μM fMD-D2$^{3-11}$-GST that was preincubated with either 1 μM of *Ec*PDF$_{His6}$ or catalytically inactive *Ec*PDF$^{E134A}_{His6}$. *D*, same as (*C*), but with fPgd1$_{HA-His6}$ instead of fMD-D2$^{3-11}$-GST. *E*, immunoblotting with anti-fMet^{Hs} and purified unformylated MD-D2-GST (0.2 μg) or Nt-formylated fMD-D2-GST (0.2 μg) in the presence of 10 mM Met, fMet, or AcMet amino acids. The *bottom* immunoblot with anti-GST indicates equal amounts of loaded proteins. *F*, immunoblotting with anti-fMet^{Hs} and serially diluted MD-D2-GST or Nt-formylated fMD-D2-GST. *G*, same as (*F*), but with Pgd1$_{HA-His6}$ or Nt-formylated fPgd1$_{HA-His6}$. *A–F* images are representative of two independent experiments. *Ec*PDF, *Escherichia coli* peptide deformylase; fMet, N-formyl methionine; Nt-, Nα-terminal.

ribosomes in human cells can produce Nt-formylated native proteins as observed in yeast cells (13).

Because the levels of Nt-formylated proteins in yeast cells are drastically influenced by environmental and intrinsic stressors (13), we hypothesized that pathophysiological perturbations might modulate the expression patterns of Nt-formylated proteins in human cells. To test this hypothesis, we measured Nt-formylated proteins by anti-fMet^{Hs}-based immunoblotting in a set of human cell lines, including HEK293 (embryonic kidney), HeLa (cervical carcinoma), MHCC97H (hepatocellular carcinoma), SW480 and HT29 (colorectal carcinoma), T24 and TCC (bladder carcinoma), and MDA231 and T47D (breast carcinoma) (Fig. 5*A*). Among them, strong upregulation of Nt-formylated proteins was observed in SW480 colon cancer cells, although each cell line exhibited different patterns with respect to the kinds of Nt-formylated proteins and their expression levels (Fig. 5*A*). Moreover, the treatment of PDF inhibitor actinonin dramatically increased the levels of Nt-formylated native proteins in SW480 cells, further verifying their retention of deformylatable fMet (Fig. 5*B*). Notably, these results also suggested that the detected fMet-containing proteins were most likely a mixture of mitochondrial DNA-encoded native proteins synthesized by mitochondrial ribosomes and nuclear DNA-encoded native

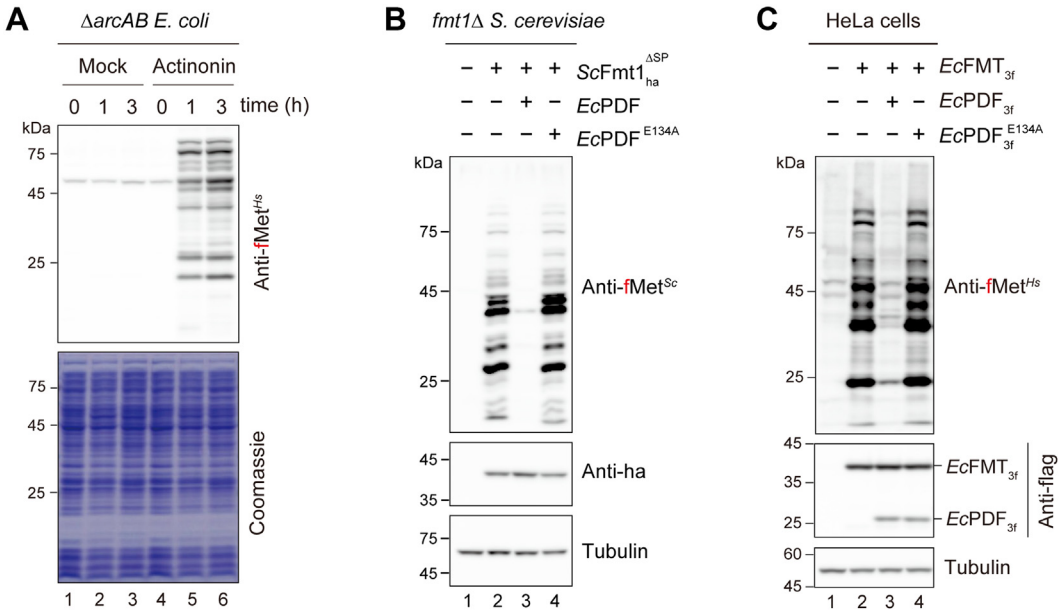

Figure 4. Detection of Nt-formylated native proteins in *E. coli*, *S. cerevisiae*, and HeLa cells. *A*, immunoblotting with anti-fMet^{Hs} and extracts of *ΔarcAB E. coli* cells that were incubated in the either presence or absence of actinonin (2 μg/ml) for 0, 1, and 3 h. The *bottom* gel with Coomassie brilliant blue staining indicates equal amounts of loaded samples. *B*, immunoblotting with anti-fMet^{Sc} purified by negative selection with extracts of *fmt1Δ S. cerevisiae* cells that expressed *SCFmt1*$^{\Delta SP}_{ha}$ together with *Ec*PDF or *Ec*PDF^{E134A}. *C*, immunoblotting with anti-fMet^{Hs} and extracts (~μg) of HeLa cells that expressed *Ec*FMT$_{3f}$ together with either *Ec*PDF$_{3f}$ or *EcPDF*$^{E134A}_{3f}$. *A–C* images are representative of two independent experiments. *Ec*PDF, *Escherichia coli* peptide deformylase; fMet, N-formyl methionine; FMT, methionyl-tRNA formyltransferase; Nt-, Nα-terminal.

proteins synthesized by cytosol ribosomes, considering that the human mitochondrial genome encodes only 13 proteins (33). Moreover, immunoblotting with anti-fMet following subcellular fractionation indicated that Nt-formylated proteins were present in both the cytosolic and mitochondrial fractions of SW480 cells (Fig. 5*C*).

Next, we employed an integrated Nt-peptide enrichment method followed by liquid chromatography–tandem mass spectrometry (LC–MS/MS) (34) to further probe the cytosolic production of Nt-formylated proteins in SW480 cells. The resulting Nt-proteome analysis identified the following Nt-formylated proteins: unconventional myosin MYO18A, tRNA splicing nuclease subunit TSEN54, non-POU domain octamer binding NONO, spectrin α chain SPTAN1, proteasome regulatory subunit PSMD2, Ser/Arg-rich splicing factor SRSF3, and tumor protein TPD52L2 (Figs. 5*D* and S2). Because those Nt-formylated proteins are nuclear DNA encoded and are therefore synthesized by cytosolic ribosomes, we concluded that Nt-formylated proteins can be endogenously produced even in the cytosol of human cells.

Discussion

In this study, we successfully generated a pan-fMet–specific polyclonal antibody that recognizes fMet-containing proteins from bacteria to humans universally and sequence or context independently (Figs. 1–5). To the best of our knowledge, anti-fMet is the first pan-specific antibody that allows the monitoring of fMet-bearing proteomes. Anti-fMet may be an invaluable resource to functionally and mechanistically elucidate poorly understood Nt-formylated proteins in various organisms. For example, bacterial Nt-formylated proteins are the product of an incomplete deformylation process and are frequently produced in *E. coli*, *Bacillus subtilis*, *Staphylococcus aureus*, and *Streptococcus pneumoniae* (12, 16, 22). In particular, ~5% of *E. coli* proteins, most of which are membrane proteins, contain the formyl moiety at their N-terminus (22). Therefore, anti-fMet may be very useful to determine their incomplete deformylation processes and functions linked to protein misfolding, membrane defects, and metabolic changes (35, 36).

fMet-containing proteins were previously shown to be produced by cytosolic ribosomes of the simple eukaryotic yeast *S. cerevisiae* (13). However, their production in multicellular organisms has remained unexplored until this study (Figs. 4*C* and 5). Thus, the observation of various Nt-formylated proteins in human cells suggests that cytosolic synthesis of Nt-formylated proteins is universal and conserved across eukaryotic species.

The various expression patterns of Nt-formylated proteins in cancer cell lines (Fig. 5*A*) may represent the previously unexplored regulation of fMet-bearing protein synthesis and their degradation by a putative mammalian fMet/N-degron pathway that remains to be identified. In particular, cytosolic production of Nt-formylated proteins may be influenced by the levels of cytosolic 10-formyltetrahydrofolate (required for Nt-formylation), mitochondrial methionyl-tRNA formyl transferase, and peptide deformylase under various stress conditions.

The current anti-fMet polyclonal antibody is available only as a finite supply. Nonetheless, the successful strategy for the first generation of a pan-fMet-specific antibody used in this study can be applied to the development of pan-fMet monoclonal antibodies and structure-based engineered nanobodies. The

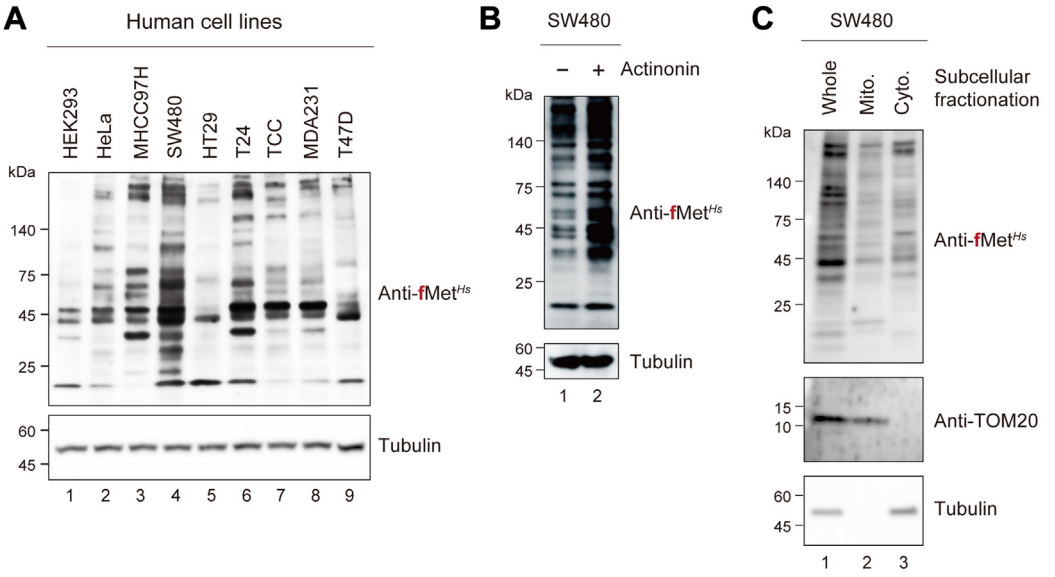

D Identified Nt-formylated proteins from SW480 colon cancer cells

Gene	Identified Nt-formylated peptide	Protein
MYO18A	fMFNLMKKDKDKDGGRKEKKEKKEKKER	Unconventional myosin-XVIIIa
TSEN54	fMEPEPEPAAVEVPAGR	tRNA-splicing nuclease subunit Sen54
NONO	fMQSNKTFNLEKQNHTPR	Non-POU domain octamer binding protein
SPTAN1	fMDPSGVKVLETAEDIQER	Spectrin alpha, non-erythrocytic 1
PSMD2	fMEEGGRDKAPVQPQQSPAAAPGGTDEKPSGKER	26S proteasome non-ATPase regulatory subunit 2
SRSF3	fMHRDSCPLDCKVYVGNLGNNGNKTELER	Ser/Arg-rich splicing factor 3
TPD52L2	fMDSAGQDINLNSPNKGLLSDSMTDVPVDTGVAAR	Tumor protein D54

Figure 5. Detection of endogenous Nt-formylated native proteins in various human cell lines. *A*, immunoblotting with anti-fMet^{Hs} and extracts (15 μg) of HEK293 (embryonic kidney), HeLa (cervical carcinoma), MHCC97H (hepatocellular carcinoma), SW480 and HT29 (colorectal carcinoma), T24 and TCC (bladder carcinoma), and MDA231 and T47D (breast carcinoma) cells. *A* images are representative of three independent experiments. *B*, immunoblotting with anti-fMet^{Hs} and extracts (15 μg) of SW480 cells that were incubated in either the absence or presence of actinonin (10 μg/ml) for 3 h before cell lysis. Immunoblot with anti-tubulin was used as a loading control. *C*, subcellular fractions of SW480 cells, followed by immunoblotting with anti-fMet^{Hs}, anti-TOM20, and anti-tubulin. TOM20 and tubulin were used as cell compartment–specific markers for the mitochondrial and cytosolic fractions, respectively. *B* and *C* images are both representative of two independent experiments. *D*, identified fMet-containing protein from SW480 cells using Nt-peptide enrichment and subsequent LC-MS/MS. See also main text and Fig. S2. fMet, N-formyl methionine; Nt-, Nα-terminal.

development of pan-fMet antibodies will greatly expand the resources to study Nt-formylated proteins that remain to be explored in terms of their physiological and pathological roles.

Experimental procedures

Reagents and antibodies

Methionine (64319), *N*-formyl methionine (F3377), *N*-acetyl methionine (01310), Sulfo-SMCC (M6035), and protease inhibitor cocktail tablets (04693132001) were purchased from Sigma-Aldrich. Affi-Gel 10/15 resins (1536099/1536051), 4 to 20% Mini-PROTEAN TGX Precast Protein Gels (4561096), and Clarity Western ECL substrate (170-5061) were purchased from Bio-Rad. Pierce RIPA buffer (89900), RPMI-1640 (11875093), and Opti-MEM (31985070) were purchased from Thermo Fisher Scientific. Dulbecco's modified Eagle's medium (DMEM) (SH30243.01), McCoy's 5a medium (SH30200.01), and fetal bovine serum (FBS) (SH30919.03) were purchased from Cytiva. Glutathione Sepharose 4B (17-0756-05) was purchased from GE Healthcare. A polypropylene column (34964), Ni-NTA agarose (30230), and Qproteome mitochondria isolation kit (37612) were purchased from Qiagen. ProA agarose (101005) was purchased from Amicogen, and actinonin (HY-113952) was purchased from MedChemExpress.

Commercial primary antibodies used in this study: anti-flag M2 monoclonal (F3165, 1:2000), anti-ha monoclonal (H9658, 1:2000), and anti-α-tubulin monoclonal (T5168, 1:2000) were purchased from Sigma-Aldrich. Anti-his-tag monoclonal (SC-8036, 1:1000), anti-GST monoclonal (SC-374171, 1:2000), and anti-TOM20 monoclonal (SC-17764, 1:500) were purchased from SCBT. HRP-conjugated secondary antibodies: goat anti-rabbit IgG (170-6515, 1:5000) and anti-mouse IgG (170-6516, 1:10,000) were purchased from Bio-Rad.

E. coli *and yeast strains, and human cell lines*

E. coli and S. cerevisiae strains and human cell lines used in this study are listed in Table 1.

Table 1
E. coli, *S. cerevisiae*, and human cells used in this study

Names	Genotypes or descriptions	Source	Catalog #
BL21(DE3)	A T7 expression *E. coli* strain	Lab collection	N/A
AG100a	*ΔacrAB* BL21(DE3)	(40)	N/A
CHY3222	*fmt1Δ::KanMX6 in* BY4741	Lab collection	N/A
HEK293	Human embryonic kidney	ATCC	CRL-1573
HeLa	Human cervical carcinoma	ATCC	CCL-2
MHCC97H	Human hepatocellular carcinoma	Lab collection	N/A
SW480	Human colorectal carcinoma	KCLB	10228
HT29	Human colorectal carcinoma	ATCC	HTB-38
T24	Human bladder carcinoma	ATCC	HTB-4
TCC	Human bladder carcinoma	ATCC	HTB-5
MDA231	Human breast carcinoma	ATCC	HTB-26
T47D	Human breast carcinoma	ATCC	HTB-133

Plasmid construction

The plasmids and primers used in this study are listed in Tables 2 and 3. To construct pCH2222, the DNA encoding $Pgd1_{HA}$ was PCR-amplified from pCH3401 using primer pair OCH1825/OCH3473, digested with *Nde*I/*Xho*I, and then ligated into *Nde*I/*Xho*I-cut pET23a(+). For the construction of pCH2248, the DNA encoding *Ec*PDF was PCR-amplified from pCH5109 using primer pair OCH2374/OCH2395, digested with *Nde*I/*Xho*I and then ligated into *Nde*I/*Xho*I-cut pET23a(+). To create pCH2249, the DNA encoding *Ec*PDF^{E134A} was PCR-amplified from pCH5110 using a primer pair, OCH2374/OCH2395, digested with *Nde*I/*Xho*I, and then inserted into *Nde*I/*Xho*I-cut pET23a(+).

To construct pCH2758, a pair of primers OCH2800/OCH2801 encoding the HA epitope tag was annealed and then inserted into *Bam*HI/*Spe*I-digested pCH3351. To construct pCH3391, the DNA fragment carrying P_{ADH1}-*EcPDF*-T_{TEF1} was retrieved from *Not*I/*Sal*I-cut pCH5109 and then ligated into *Not*I/*Sal*I-cut pRS315. To construct pCH3392, the DNA fragment carrying P_{ADH1}-*EcPDF*^{E134A}-T_{TEF1} was retrieved from *Not*I/*Sal*I-digested pCH5110 and then inserted into *Not*I/*Sal*I-digested pRS315.

For the construction of pCH5537, *EcFMT* DNA was amplified by PCR from pCH3323 using primer pair OCH3490/5573, and *3×FLAG* DNA was generated by overlapping PCR using primer pair OCH5576/5577. *EcFMT* and *3×FLAG* PCR products were used as templates for overlapping extension PCR with primer pair OCH3490/OCH5577. The resulting PCR product was digested with *Kpn*I/*Xho*I and then ligated into *Kpn*I/*Xho*I-digested pcDNA3(+). To construct pCH5540, *EcPDF* DNA was amplified by PCR from pCH5109 using primer pair OCH5574/5575. Then, *EcPDF and 3×FLAG* PCR products were used as templates for overlapping extension PCR with primer pair OCH5574/OCH5577. The resulting PCR product was digested with *Kpn*I/*Xho*I and then ligated into *Kpn*I/*Xho*I-digested OGS411. To construct pCH5541, *EcPDF*^{E134A} *DNA* was amplified by PCR from pCH5110 using primer pair OCH5574/5575. *EcPDF*^{E134A} and *3×FLAG* DNAs were used as templates for overlapping extension PCR with primer pair OCH5574/OCH5577. The resulting PCR product was digested with *Kpn*I/*Xho*I and then ligated into *Kpn*I/*Xho*I-digested OGS411. All final plasmid constructs were confirmed by DNA sequencing.

Preparation of yeast cell extracts for Affi-Gel 10/15 chromatography

Fmt1Δ S. cerevisiae (*fmt1Δ::kanMX6* in BY4741) cells were grown at 30 °C to A_{600} = ∼1.0 in 600 ml YPD (1% yeast extract, 2% peptone, and 2% glucose) medium and then centrifugated at 2000*g* for 15 min at 4 °C. After washing twice in ice-cold phosphate-buffered saline (PBS) (137 mM NaCl, 2.7 mM KCl, 10 mM Na_2HPO_4, and 1.8 mM KH_2PO_4), the pellets were resuspended in 15 ml lysis buffer *A* (20 mM Hepes, pH 7.5, 150 mM NaCl, 0.5 mM Na-EDTA, 1% Triton X-100, 1 mM DTT, 1 mM PMSF, 10% glycerol, and 1× protease inhibitor cocktail) and disrupted with a Mini-Beadbeater-24 (BioSpec Products); this was done four times for 15 s each with a 1 min interval on ice. After centrifugation at 12,000*g* for 15 min at 4 °C, the supernatants were dialyzed against the conjugation buffer (20 mM Hepes, pH 7.6, 100 mM NaCl, 0.5 mM EDTA, 10% glycerol, 0.1 mM PMSF, 1 mM DTT, and 0.1% NP-40) at 4 °C for 4 h, followed by re-dialysis against fresh conjugation buffer for 2 h. After centrifugation of the samples at 12,000*g* for 10 min at 4 °C, the supernatants were stored for conjugation to Affi-Gel 10/15 resins as described below.

Preparation of HeLa cell extracts for Affi-Gel 10/15 chromatography

HeLa cells were seeded at 3 × 10^6 cells per plate in 40 × 10 cm cell culture plates (SPL Life Sciences) in DMEM

Table 2
Plasmids used in this study

Plasmids	Description	Source
pET23a(+)	Bacterial expression vector with a T7 promoter	Lab collection
pRS315	CEN-based yeast vector with a *LEU2* marker	Lab collection
pRS316	CEN-based yeast vector with a *URA3* marker	Lab collection
pcDNA3(+)	Mammalian expression vector with a CMV promoter	Lab collection
OGS411	Mammalian expression vector with dual CMV promoters	Sigma-Aldrich
pCH2218	MD-$D2^{3-11}$-GST in pET23a(+)	(13)
pCH2222	$Pgd1_{Ha\text{-}His6}$ in pET23a(+)	This study
pCH2248	$Ec PDF_{His6}$ in pET23a(+)	This study
pCH2249	*EcPDF*$^{E134A}_{His6}$ *in pET23a(+)*	This study
pCH2758	P_{TDH3}-*Sc*FMT1(27-401)$_{Ha}$-T_{CYC1} in pRS316	This study
pCH3323	P_{ADH1}-*Ec*FMT-T_{CYC1} in pRS316	(13)
pCH3351	P_{TDH3}-*Sc*FMT1(27-401)-yeGFP-T_{CYC1} in pRS316	(13)
pCH3391	P_{ADH1}-*Ec*PDF-T_{TEF1} in pRS315	This study
pCH3392	P_{ADH1}-*Ec*PDF^{E134A}-T_{TEF1} in pRS315	This study
pCH3402	P_{CUP1}-$Pgd1_{Ha}$-T_{ADH1} and P_{ADH1}-T_{CYC1} in pRS314	(13)
pCH5109	P_{ADH1}-*Ec*PDF-T_{TEF1} in pRS314	(13)
pCH5110	P_{ADH1}-*Ec*PDF^{E134A}-T_{TEF1} in pRS314	(13)
pCH5537	P_{CMV}-*Ec*FMT_{3f} in pcDNA3(+)	This study
pCH5540	P_{CMV1}-*Ec*PDF_{3f} and P_{CMV2} in OGS411	This study
pCH5541	P_{CMV1}-*EcPDF*$^{E134A}_{3f}$ *and* P_{CMV2} *in OGS411*	This study

Table 3
Primers used in this study

Names	Primer sequences
OCH1825	5′-AATCTCGAGAGCGTAATCTGGAACATC-3′
OCH2394	5′-AATCATATGTCAGTTTTGCAAGTGTTACAT-3′
OCH2395	5′-AATCTCGAGAGCCCGGGCTTTCAGACG-3′
OCH2800	5′-GATCCTACCCATACGACGTCCCA-GATTACGCCTAAA-3′
OCH2801	5′-CTAGTTTAGGCGTAATCTGGGACGTCGTATGGG-TAG-3′
OCH3473	5'-ATACATATGGACTCGATTATACCGGCAGGCGTC-3'
OCH3490	5′-ATAGGTACCATGTCAGAATCACTACGTATT-3′
OCH5573	5′-TGGTCTTTGTAGTCGAATTCGACCA-GACGGTTGCCCGG-3′
OCH5574	5′-AATGGTACCATGTCAGTTTTGCAAGTG-3′
OCH5575	5′-TGGTCTTTGTAGTCGAATTCAGCCCGGGCTTTCA-GACG-3′
OCH5576	5′-AATTCGACTACAAAGACCATGACGGTGATTA-TAAAGATCATGACATCGACTA-3′
OCH5577	5′-AATCTCGAGTCACTTGTCATCGTCATCCTTG-TAGTCGATGTCATGATCTTTA-3′

supplemented with 10% FBS. After 24 h of culture (70% confluence), the HeLa cells were transfected with pCH5540 expressing *E. coli* PDF using polyethylenimine. At 36 h after transfection, the cells were washed with ice-cold PBS and collected by a cell scraper (SPL Life Sciences). The harvested cells were resuspended in 15 ml lysis buffer *B* (50 mM Tris HCl, pH 7.6, 150 mM NaCl, 1% NP-40, 1 mM DTT, and 1× proteasome inhibitor cocktail) and incubated on ice for 30 min. After sonication (60 repeats of a 1 s pulse and 1 s rest with a 30% amplitude on ice), the cell lysates were centrifuged at 12,000*g* for 10 min at 4 °C. The supernatants were dialyzed against the conjugation buffer as described above to prepare HeLa cell lysates.

Affi-Gel 10/15 resins derivatized with yeast or human cell extracts

Equal volumes of Affi-Gel 10 (1 ml) and Affi-Gel 15 (1 ml) were mixed and then loaded into a polypropylene column. The resins were washed with 10 ml PBS, incubated with 7.5 ml of the above yeast or HeLa lysate (>20 mg per column) at 4 °C for ∼16 h with gentle rotating, and then the unconjugated sample was drained from the column. After washing with 5 ml PBS, 10 ml blocking buffer (1 M Tris HCl, pH 7.6) was applied on the resins, and the column was rotated at 4 °C for 2 h. After draining the blocking buffer, the column was washed with 10 ml washing buffer (1 M NaCl) and then with 10 ml PBS. For long-term storage, the resins were soaked with 2 ml storage buffer [PBS with 0.05% NaN_3 (w/v)].

Generation of anti-fMet^{Hs} and anti-fMet^{Sc}

The Nt-formylated synthetic peptide fMGSGC was conjugated to the keyhole limpet hemocyanin carrier *via* its C-terminal Cys. Sulfo-SMCC (Sigma-Aldrich) was used as a conjugation linker between the peptide and the carrier. Rabbit polyclonal antisera against the antigen peptide were produced *via* primary antigen injection at week 0, boosting at week 4, 6, and 8, and final heart puncture at week 9. The antisera production was conducted by AbClon. Anti-fMet antisera specific for Nt-formylated proteins were negatively selected by incubating 2 ml of the raised sera with Affi-Gel 10/15 resins derivatized with total proteins extracted from *fmt1Δ S. cerevisiae* or *Ec*PDF-expressing HeLa cells. To maximally remove nonspecific antisera against Nt-unformylated proteins, the negative selection procedures were repeated five or three times with the *fmt1Δ* yeast or PDF-expressing HeLa cell extracts, respectively.

The flowthroughs of antisera were incubated with 0.5 ml ProA-Sepharose (Amicogen) at 4 °C for 4 h with gentle rotation. Then, the bound antibodies were washed with 10 ml PBS and eluted with 0.25 ml elution buffer (0.3 M glycine, pH 3.0). The resulting antibodies were immediately neutralized by adding 60 μl of 1 M Tris HCl (pH 7.6). After repeating the elution–neutralization steps three times, the collected antibodies were dialyzed against storage buffer at 4 °C for ∼16 h and again at 4 °C for ∼4 h after exchanging the storage buffer. The final products were named anti-fMet^{Hs} or anti-fMet^{SC} in accordance with the negative selection extracts.

SPOT binding assay with anti-fMet^{Hs}

A set of synthetic XZ-D2$^{3-11}$ peptides (X = Met, fMet, AcMet; Z = any 20 amino acids) was employed for this assay. The designed peptides were C-terminally linked to a cellulose-PEG membrane as dots. Except for varying residues at positions 1 and 2, 3 to 11 residues of SPOT-arrayed peptides were identical to the Nt-sequence of the previously characterized D2 protein (see main text). The peptides were synthesized by JPT. The SPOT membrane was soaked in methanol for 5 min, washed three times with PBS-T [PBS with 0.1% Tween 20 (w/v)] for 5 min and then blocked with Super block T20 (Thermo Fisher Scientific) at 4 °C for ∼16 h. Anti-fMet antibody was diluted in Super block T20 (final concentration of 2 μg/ml). The membrane was incubated with anti-fMet^{Hs} at 4 °C for ∼16 h and then washed three times with PBS-T for 5 min each. After 2-h incubation with an HRP-conjugated goat anti-rabbit secondary antibody (1:5000 diluted in Super block T20) at RT, the membrane was washed three times with PBS-T for 5 min each. Signals were developed with ECL substrates in chemiluminescence mode using GE Amersham Imager AI680.

Dot blot with anti-fMet^{Hs}

The indicated peptides were synthesized by Peptron. The indicated amounts of peptides were serially diluted in distilled water and dotted on a nitrocellulose (NC) membrane with a 0.2 nm pore size. After drying at RT, the NC membrane was blocked for 1 h with blocking solution (5% dry skim milk in PBS-T). After brief washing with PBS-T twice, the NC membrane was incubated with the anti-fMet^{Hs} antibody (final concentration of 2 μg/ml) in PBS-T at 4 °C for ∼16 h. After washing three times with PBS-T for 5 min each, the membrane was incubated with a secondary goat anti-rabbit IgG antibody (1:5000 diluted in PBS-T) for 1 h at RT. After washing three times with PBS-T, the membranes were soaked in ECL substrate solution and then developed in chemiluminescence mode using the GE Amersham Imager AI680.

Purification of MD-D2$^{3-11}$-GST, fMD-D2$^{3-11}$-GST, Pgd1$_{HA\text{-}His6}$, fPgd1$_{HA\text{-}His6}$, Ec*PDF*$_{His6}$, and Ec*PDF*$^{E134A}_{His6}$

AG100a (*ΔarcAB*) *E. coli* cells were transformed with plasmids expressing the indicated fusion proteins. Then, a 10 ml overnight culture of the transformed cells was inoculated into 500 ml LB medium containing 100 μg/ml ampicillin. The cells were grown at 37 °C to A_{600} = ∼0.6. Expression of the indicated fusions was induced in *E. coli* cells by addition of IPTG (0.5 mM final concentration) and subsequent culture at 30 °C for 4 h. To express Nt-formylated fMD-D2$^{3-11}$-GST or fPgd1$_{HA\text{-}His6}$, actinonin (final concentration of 2 μg/ml) was treated together with 0.5 mM IPTG.

Purification of MD-D2$^{3-11}$-GST and fMD-D2$^{3-11}$-GST was performed using Glutathione Sepharose resin (GE Healthcare) as described previously (13). To purify Pgd1$_{HA\text{-}His6}$ and fPgd1$_{HA\text{-}His6}$, cell pellets were lysed in lysis buffer *C* (300 mM NaCl, 20 mM imidazole, and 50 mM Tris HCl, pH 7.6) containing 0.5 mg/ml lysozyme, 1 mM PMSF, and 0.5 mM DTT. After incubation on ice for 20 min, the cells were disrupted by sonication (60 times for a 1 s pulse and 1 s rest with a 30% amplitude). After centrifugation at 12,000*g* for 20 min at 4 °C, clear cell lysates were obtained and bound to 0.5 ml Ni-NTA agarose at 4 °C for 4 h. Protein-bound Ni-NTA resin was washed with lysis buffer *C* with 0.5 mM DTT and then with Ni-NTA washing buffer (300 mM NaCl, 50 mM imidazole, and 50 mM Tris HCl, pH 7.6). The proteins were eluted by applying 0.5 ml Ni-NTA elution buffer (300 mM NaCl, 500 mM imidazole, and 50 mM Tris HCl, pH 7.6) three times, followed by overnight dialysis against dialysis buffer (10% glycerol, 150 mM NaCl, 10 mM β-mercaptoethanol, and 50 mM Tris HCl, pH 7.6). *Ec*PDF$_{His6}$ and *EcPDF*$^{E134A}_{His6}$ were purified from BL21 *E. coli* cells carrying pCH2248 or pCH2249 in accordance with the purification procedures for Pgd1$_{HA\text{-}His6}$ as described above.

In vitro *protein deformylase assay*

1 μM fMD-D2$^{3-11}$-GST or fPgd1$_{HA\text{-}His6}$ was preincubated with *Ec*PDF$_{His6}$ or *EcPDF*$^{E134A}_{His6}$ in deformylase reaction buffer (50 mM Hepes pH 7.6, 500 mM KCl, and 1 mM DTT). After incubation at 30 °C for 1 h, the reaction mixtures were subjected to immunoblotting with anti-fMet^{Hs}.

Amino acid competition assay

0.2 μg MD-D2$^{3-11}$-GST or fMD-D2$^{3-11}$-GST was subjected to immunoblotting with anti-fMet^{Hs}. Specifically, we added 10 mM of fMet, Met, or AcMet amino acid to PBS-T solution containing anti-fMet^{Hs} (final concentration of 2 μg/ml) before immunoblotting with anti-fMet^{Hs}.

Immunoblotting of E. coli, S. cerevisiae, *and human cell extracts with anti-fMet*^{Hs} *or anti-fMet*^{Sc}

AG100a E. coli cells (10 ml) were cultured in LB medium to A_{600} = ∼0.6 and then treated with 1 μl of ethanal (EtOH) only (mock) or actinonin (20 mg/ml in EtOH). At certain time points, 1.5 ml cells were harvested by centrifuging at 12,000*g* for 2 min at 4 °C. The resulting cell pellets were lysed with lysis buffer *D* (2% SDS with 1× protease inhibitor cocktail), followed by brief sonication and centrifugation at 12,000*g* for 10 min at 4 °C. After collecting the supernatants, the protein concentration was determined using a BCA protein assay. Then, the collected supernatants were diluted to 2 μg/μl in lysis buffer *D*, mixed with 4× SDS sample buffer at a 3:1 ratio, and heated at 70 °C for 10 min. Then, 7 μl of each sample was subjected to immunoblotting with anti-fMet^{Hs} and Coomassie brilliant blue staining. Immunoblots were developed with ECL substrate in chemiluminescence mode using the GE Amersham Imager AI680.

To prepare yeast samples, CHY3222 (*fmt1Δ* in BY4741) cells were, using the LiAc/SS carrier DNA/PEG method (37), cotransformed with a pair of the following plasmids: pRS316/pRS315, pCH2758/pRS315, pCH2758/CH3391, or pCH2758/pCH3392. Each transformant was inoculated and grown in synthetic complete medium (SC-Leu/-Ura) (0.17% yeast nitrogen base without amino acids, 0.5% ammonium sulfate, 2% glucose, and 0.6% complete supplement mixture without leucine and uracil) at 30 °C. When grown to A_{600} = ∼1, the yeast cells equivalent to 1.2 ml of cell suspension at A_{600} = 1 were harvested by centrifugation at 12,000*g* for 1 min. The cell pellets were resuspended in 1 ml of 0.2 N NaOH and incubated on ice for 20 min. After centrifugation at 12,000*g* at 4 °C for 1 min, the pelleted cells were resuspended in 50 μl HU buffer (8 M urea, 5% SDS, 1 mM Na-EDTA, 0.1 M DTT, 0.01% bromophenol blue, 0.2 M Tris HCl, pH 6.8, and 1× protease inhibitor cocktail). After heating at 70 °C for 10 min, the samples were centrifuged for 5 min at 12,000*g*. The supernatants were collected and subjected to immunoblotting with anti-fMet^{Sc}, anti-HA, and anti-tubulin.

To prepare extracts of HeLa cells, HeLa cells were seeded on 12-well culture plates (2 × 10^5 cells per well), grown to 70% confluence, and cotransfected with a set of plasmid pairs (0.35 μg each), pcDNA3/OGS411, pCH5537/OGS411, pCH5537/pCH5540, or pCH5537/pCH5541, using 2.5 μl polyethylenimine solution (1 mg/ml). Cells were harvested after transfection of 36 h in 2× SDS sample buffer. Samples were sonicated briefly, heated at 70 °C for 10 min, and then subjected to immunoblotting with anti-fMet^{Hs}, anti-flag, or anti-tubulin.

To prepare extracts from human cell lines, each cell line was cultured in the appropriate medium: HEK293, HeLa, MHCC97H, HT29, and MDA231 in DMEM + 10% FBS, SW480, TCC, and T47D in RPMI-1640 + 10% FBS and T24 in McCoy's 5a medium + 10% FBS. Cells were harvested by trypsinization. Cell pellets were resuspended in RIPA buffer containing a protease inhibitor cocktail and 20 μg/ml actinonin. After incubation on ice for 20 min, cell lysates were sonicated briefly and centrifuged at 12,000*g* for 10 min at 4 °C. The collected supernatants were diluted to 2 μg/μl in RIPA buffer, mixed with 4× SDS sample buffer at a 3:1 ratio, and heated at 70 °C for 10 min. Then, 10 μl of each sample was subjected to immunoblotting with anti-fMet^{Hs} and anti-tubulin.

For actinonin treatment, SW480 cells were grown to 70% confluency in 2 ml of RPMI + 10% FBS, treated with 1 μl of

Detection of Nt-formylated native proteins

EtOH only (mock) or actinonin (20 mg/ml in EtOH), and incubated for 3 h before cell lysis. Subcellular fractionation of SW480 cells was performed using Qproteome mitochondria isolation kit (Qiagen). Then, 10 μg of whole cell lysates and 2.5 μg of the mitochondrial and cytosolic fractions were subjected to immunoblotting with anti-fMet^{Hs}, anti-TOM20, and anti-tubulin.

Nt-peptide analyses

SW480 cells were first lysed in lysis buffer *E* [0.2 M EPPS pH 8.0, 6 M guanidine, 10 mM TCEP, 40 mM 2-chloroacetamide, and 1× Halt Protease Inhibitor (Thermo Fisher Scientific)]. Nt-peptides were enriched from 100 μg protein *via* the integrated Nt-peptide enrichment method and then analyzed using LC-MS/MS as previously described (34). Raw spectral files were converted with MSconvert (38), and a database search was performed with MS-GF+ program (39) against the UniProt human reference proteome database (release 2018_07) and the additional common contaminant database cRAP (https://www.thegpm.org/crap/). With respect to modifications, carbamidomethyl (+56.021464 Da) on Cys and D3-acetyl (+45.029395 Da) on Lys were set as fixed, and oxidation (+15.994915 Da) on Met, acetyl (+42.010565 Da), formyl (+27.994915 Da), pyroglutamation (−18.010565 Da), and dimethyl (+28.031300 Da) on peptide N terminus and dimethyl on Arg and Asn were set as variable. Identifications were filtered with a 1% false discovery rate.

Data availability

The mass spectrometry proteomics data reported here were deposited to the ProteomeXchange Consortium *via* the PRIDE partner repository with the dataset identifier PXD039053 and DOI 10.6019/PXD039053. The raw proteomics data were also deposited in K-BDS (Korea BioData Station, https://kbds.re.kr) with the accession ID PRJKA230528. All data are available in the main text and the supporting information. Further details are also available upon reasonable request.

Supporting information—This article contains supporting information. (13, 14)

Acknowledgments—We thank Y. Lee (POSTECH, Pohang, South Korea) for human cell lines and R. Sauer (MIT, Cambridge, MA, USA) for AG100A *E coli*. We also thank present and former members of the Hwang laboratory for their advice and assistance. We thank M. Arico from Edanz (https://www.edanz.com/ac) and H. Jose from Enago (www.enago.co.kr) for editing a draft of this article.

Author contributions—D. K., J.-M. K., C. L., and C.-S. H conceptualization; D. K., O.-H. S., S. J., S.-Y. K., J.-M. K., C. L., and C.-S. H. methodology; D. K., O.-H. S., S. J., S.-Y. K., J.-M. K., C. L., and C.-S. H investigation; D. K., O.-H. S., S. J., S.-Y. K., and J.-M. K. data curation; D. K., S. J., C. L., and C.-S. H. formal analysis; D. K., S. J., and C.-S. H. writing–original draft; D. K., S. J., and C.-S. H. writing–review and editing; D. K. S. J., O.-H. S., and C.-S. H. resources; J.-M. K., C. L., and C.-S. H. supervision; J.-M. K., C. L., and C.-S. H. funding acquisition.

Funding and additional information—This study was supported by grants from the Korean Government (MSIP), NRF-2020R1A3B2078127 and NRF-2017R1A5A1015366 (to C.-S. H.), NRF-2020R1C1C1012386 (to J.-M. K.), and NRF-2022M3H9A2096187 and NRF-2021R1A6A3A01088437 (to C. L.). This study was also supported by a Korea University Grant.

Conflict of interest—All authors declare no conflict of interest with the contents of this article.

Abbreviations—The abbreviations used are: fMet, N-formyl methionine; fMGSGC, fMet-Gly-Ser-Gly-Cys; FMT, methionyl-tRNA formyl transferase; Nt-, Nα-terminal; PDF, peptide deformylase.

References

1. Clark, B. F., and Marcker, K. A. (1966) The role of N-formyl-methionyl-sRNA in protein biosynthesis. *J. Mol. Biol.* **17**, 394–406
2. Adams, J. M., and Capecchi, M. R. (1966) N-formylmethionyl-sRNA as the initiator of protein synthesis. *Proc. Natl. Acad. Sci. U. S. A.* **55**, 147–155
3. Guillon, J. M., Mechulam, Y., Schmitter, J. M., Blanquet, S., and Fayat, G. (1992) Disruption of the gene for Met-tRNA(fMet) formyltransferase severely impairs growth of *Escherichia coli*. *J. Bacteriol.* **174**, 4294–4301
4. Wu, X. Q., and RajBhandary, U. L. (1997) Effect of the amino acid attached to *Escherichia coli* initiator tRNA on its affinity for the initiation factor IF2 and on the IF2 dependence of its binding to the ribosome. *J. Biol. Chem.* **272**, 1891–1895
5. Smith, A. E., and Marcker, K. A. (1968) N-formylmethionyl transfer RNA in mitochondria from yeast and rat liver. *J. Mol. Biol.* **38**, 241–243
6. Leis, J. P., and Keller, E. B. (1970) Protein chain-initiating methionine tRNAs in chloroplasts and cytoplasm of wheat leaves. *Proc. Natl. Acad. Sci. U. S. A.* **67**, 1593–1599
7. Schmitt, E., Panvert, M., Blanquet, S., and Mechulam, Y. (1998) Crystal structure of methionyl-tRNAfMet transformylase complexed with the initiator formyl-methionyl-tRNAfMet. *EMBO J.* **17**, 6819–6826
8. Meinnel, T., and Blanquet, S. (1993) Evidence that peptide deformylase and methionyl-tRNA(fMet) formyltransferase are encoded within the same operon in *Escherichia coli*. *J. Bacteriol.* **175**, 7737–7740
9. Kramer, G., Boehringer, D., Ban, N., and Bukau, B. (2009) The ribosome as a platform for co-translational processing, folding and targeting of newly synthesized proteins. *Nat. Struct. Mol. Biol.* **16**, 589–597
10. Bingel-Erlenmeyer, R., Kohler, R., Kramer, G., Sandikci, A., Antolic, S., Maier, T., *et al.* (2008) A peptide deformylase-ribosome complex reveals mechanism of nascent chain processing. *Nature* **452**, 108–111
11. Meinnel, T., and Giglione, C. (2022) N-terminal modifications, the associated processing machinery, and their evolution in plastid-containing organisms. *J. Exp. Bot.* **73**, 6013–6033
12. Bandow, J. E., Becher, D., Buttner, K., Hochgrafe, F., Freiberg, C., Brotz, H., *et al.* (2003) The role of peptide deformylase in protein biosynthesis: a proteomic study. *Proteomics* **3**, 299–306
13. Kim, J. M., Seok, O. H., Ju, S., Heo, J. E., Yeom, J., Kim, D. S., *et al.* (2018) Formyl-methionine as an N-degron of a eukaryotic N-end rule pathway. *Science* **362**, 6418
14. Lee, C. S., Kim, D., and Hwang, C. S. (2022) Where does N-formylmethionine come from? What for? Where is it going? What is the origin of N-formylmethionine in eukaryotic cells? *Mol. Cells* **45**, 109–111
15. Piatkov, K. I., Vu, T. M., Hwang, C. S., and Varshavsky, A. (2015) Formylmethionine as a degradation signal at the N-termini of bacterial proteins. *Microb. Cell* **2**, 376–393
16. Bufe, B., Schumann, T., Kappl, R., Bogeski, I., Kummerow, C., Podgorska, M., *et al.* (2015) Recognition of bacterial signal peptides by mammalian formyl peptide receptors: a new mechanism for sensing pathogens. *J. Biol. Chem.* **290**, 7369–7387

17. Migeotte, I., Communi, D., and Parmentier, M. (2006) Formyl peptide receptors: a promiscuous subfamily of G protein-coupled receptors controlling immune responses. *Cytokine Growth Factor Rev.* **17**, 501–519
18. Lee, H. Y., Lee, M., and Bae, Y. S. (2017) Formyl peptide receptors in cellular differentiation and inflammatory diseases. *J. Cell Biochem.* **118**, 1300–1307
19. Hinttala, R., Sasarman, F., Nishimura, T., Antonicka, H., Brunel-Guitton, C., Schwartzentruber, J., *et al.* (2015) An N-terminal formyl methionine on COX 1 is required for the assembly of cytochrome c oxidase. *Hum. Mol. Genet.* **24**, 4103–4113
20. Arguello, T., Köhrer, C., RajBhandary, U. L., and Moraes, C. T. (2018) Mitochondrial methionyl N-formylation affects steady-state levels of oxidative phosphorylation complexes and their organization into supercomplexes. *J. Biol. Chem.* **293**, 15021–15032
21. Cai, N., Gomez-Duran, A., Yonova-Doing, E., Kundu, K., Burgess, A. I., Golder, Z. J., *et al.* (2021) Mitochondrial DNA variants modulate N-formylmethionine, proteostasis and risk of late-onset human diseases. *Nat. Med.* **27**, 1564–1575
22. Bienvenut, W. V., Giglione, C., and Meinnel, T. (2015) Proteome-wide analysis of the amino terminal status of *Escherichia coli* proteins at the steady-state and upon deformylation inhibition. *Proteomics* **15**, 2503–2518
23. Tanaka, F., Jones, T., Kubitz, D., and Lerner, R. A. (2007) Anti-formyl peptide antibodies. *Bioorg. Med. Chem. Lett.* **17**, 1943–1945
24. Grimsrud, P. A., Swaney, D. L., Wenger, C. D., Beauchene, N. A., and Coon, J. J. (2010) Phosphoproteomics for the masses. *ACS Chem. Biol.* **5**, 105–119
25. Kee, J. M., Oslund, R. C., Perlman, D. H., and Muir, T. W. (2013) A pan-specific antibody for direct detection of protein histidine phosphorylation. *Nat. Chem. Biol.* **9**, 416–421
26. Xu, W., and Zhao, S. (2013) Generation and characterization of pan-specific anti-acetyllysine antibody. *Methods Mol. Biol.* **981**, 137–150
27. Chng, J., Wang, T., Nian, R., Lau, A., Hoi, K. M., Ho, S. C., *et al.* (2015) Cleavage efficient 2A peptides for high level monoclonal antibody expression in CHO cells. *MAbs* **7**, 403–412
28. Dintzis, H., Dintzis, R., and Vogelstein, B. (1976) Molecular determinants of immunogenicity: the immunon model of immune response. *Proc. Natl. Acad. Sci. U. S. A.* **73**, 3671–3675
29. Nguyen, K. T., Ju, S., Kim, S. Y., Lee, C. S., Lee, C., and Hwang, C. S. (2022) N-terminal modifications of ubiquitin via methionine excision, deamination, and arginylation expand the ubiquitin code. *Mol. Cells* **45**, 158–167
30. Reineke, U., Volkmer-Engert, R., and Schneider-Mergener, J. (2001) Applications of peptide arrays prepared by the SPOT-technology. *Curr. Opin. Biotechnol.* **12**, 59–64
31. Rajagopalan, P. R., and Pei, D. (1998) Oxygen-mediated inactivation of peptide deformylase. *J. Biol. Chem.* **273**, 22305–22310
32. Mamelli, L., Petit, S., Chevalier, J., Giglione, C., Lieutaud, A., Meinnel, T., *et al.* (2009) New antibiotic molecules: bypassing the membrane barrier of gram negative bacteria increases the activity of peptide deformylase inhibitors. *PLoS One* **4**, e6443
33. Schon, E. A., DiMauro, S., and Hirano, M. (2012) Human mitochondrial DNA: roles of inherited and somatic mutations. *Nat. Rev. Genet.* **13**, 878–890
34. Ju, S., Kwon, Y., Kim, J.-M., Park, D., Lee, S., Lee, J.-W., *et al.* (2020) iNrich, rapid and robust method to enrich N-terminal proteome in a highly multiplexed platform. *Anal. Chem.* **92**, 6462–6469
35. Yang, C. I., Zhu, Z., Jones, J. J., Lomenick, B., Chou, T. F., and Shan, S. O. (2022) System-wide analyses reveal essential roles of N-terminal protein modification in bacterial membrane integrity. *iScience* **25**, 104756
36. Yang, C. I., Kim, J., and Shan, S. O. (2022) Ribosome-nascent chain interaction regulates N-terminal protein modification. *J. Mol. Biol.* **434**, 167535
37. Gietz, R. D. (2014) Yeast transformation by the LiAc/SS carrier DNA/PEG method. *Methods Mol. Biol.* **1163**, 33–44
38. Chambers, M. C., Maclean, B., Burke, R., Amodei, D., Ruderman, D. L., Neumann, S., *et al.* (2012) A cross-platform toolkit for mass spectrometry and proteomics. *Nat. Biotechnol.* **30**, 918–920
39. Kim, S., and Pevzner, P. A. (2014) MS-GF+ makes progress towards a universal database search tool for proteomics. *Nat. Commun.* **5**, 1–10
40. Spector, S., Flynn, J. M., Tidor, B., Baker, T. A., and Sauer, R. T. (2003) Expression of Nformylated proteins in Escherichia coli. *Protein Expr Purif.* **32**, 317–322